

## ORGANIC NITROGEN CONVERSION DURING THE THERMAL DECOMPOSITION OF HUADIAN OIL SHALE OF CHINA

XIANGXIN HAN<sup>(a)\*</sup>, BIN CHEN<sup>(a)</sup>, QINGYOU LI<sup>(a)</sup>,  
JIANHUI TONG<sup>(b)</sup>, XIUMIN JIANG<sup>(a)</sup>

<sup>(a)</sup> Institute of Thermal Energy Engineering, Shanghai Jiao Tong University, Shanghai 200240, PR China

<sup>(b)</sup> School of Materials Science and Engineering, Jingdezhen Ceramic Institute, Jingdezhen 333001, PR China

**Abstract.** Organic nitrogen plays an adverse role in the utilization of oil shale, deactivating catalysts in the shale oil refining process and forming  $\text{NO}_x$  in the combustion of oil shale and shale oil. To have a deep understanding of its thermochemical transformation during the decomposition of oil shale, the conversion of organic nitrogen is experimentally studied and a set of physical models of nitrogen-containing groups is constructed and solved using the quantum chemical transition state theory (TST) in the Gaussian 09, Revision A.02 package. The results obtained show that three principal nitrogen-containing species – pyrrolic nitrogen, pyridinic nitrogen and amino nitrogen – first crack to nitriles or amino species from the breakup of the C–N bond, and then to HCN and  $\text{NH}_3$ . If attacked by oxygen-containing groups, the nitrogen-containing products formed can be further converted into  $\text{NO}_x$ . Including also quaternary and chemisorbed  $\text{NO}_x$  in the study, the conversion history of five typical nitrogen-containing groups present in oil shale kerogen is summarized and illustrated.

**Keywords:** oil shale pyrolysis, organic nitrogen, thermochemical conversion, quantum chemistry, transition state theory.

### 1. Introduction

Nitrogen is the second most abundant heteroatom in many fossil fuels, e.g. coal, oil shale and oil tar, after oxygen [1–4]. According to previous investigations [5–7], nitrogen in oil shale kerogen mainly exists in five forms: pyrrolic nitrogen (N-5), pyridinic nitrogen (N-6), quaternary nitrogen ( $-\text{NH}_4$ ), amino nitrogen ( $-\text{NH}_2$ ) and chemisorbed  $\text{NO}_x$ . Pyrrolic nitrogen is

---

\* Corresponding author: e-mail [hanxiangxin@sjtu.edu.cn](mailto:hanxiangxin@sjtu.edu.cn)

mostly present in the form of indole and carbazole, while pyridinic nitrogen chiefly appears as pyridine, quinoline and aridine. Since organic nitrogen exerts a harmful effect on both the combustion and retorting of oil shale, it is highly necessary to more thoroughly investigate its thermochemical conversion during these processes.

Although many investigations have been carried out on nitrogen conversion during oil shale pyrolysis, most of them were conducted just from an experimental perspective [5, 8]. It is well known that the experimental method can provide some reliable clues for improving operational parameters to decrease the formation of toxic nitrogen-containing products, however, it is incapable of further disclosing the history of organic nitrogen conversion on a microcosmic level. In this respect, quantum chemistry has gained in popularity, especially after having been successfully applied to the studies of chemical conversion mechanisms of coal, providing a useful reference to explore the thermochemical conversion mechanisms of other fossil fuels on a molecular scale. For example, Zhai et al. [9] performed *ab initio* calculations using the density functional theory (DFT) to investigate the pyrolysis mechanism of pyrrole, and proposed the mechanism responsible for the formation of allyl cyanide, a major product formed during the decomposition of pyrrole. Ling et al. [10] investigated the pyrolysis mechanism of quinoline and isoquinoline using a DFT method combined with the transition state theory (TST), and obtained theoretical energy barriers for some pyrolysis reaction pathways, which were in good agreement with experimental results. Ninomiya et al. [11] studied the pyrolysis of pyridine by using semi-empirical parameterized model 3 (PM3) molecular orbitals together with TST, and made a comparison between theoretical and experimental results. Based on the above, quantum chemistry methods have proved successful in investigating the pyrolysis mechanism of coal. Considering the similarities between coal and oil shale in both physical and chemical properties, especially in nitrogen species composition [3, 12], the same methods may be applied to studying oil shale pyrolysis as well.

On the basis of the experimental results obtained from retorting Huadian oil shale, as well as its kerogen structural characteristics, this work was designed to elucidate the conversion mechanism of five main nitrogen species branched to nitrogen-containing groups during oil shale pyrolysis. The related calculations were carried out using TST in the Gaussian 09, Revision A.02 package to obtain possible conversion courses of organic nitrogen. Finally, the mechanism of nitrogen conversion during oil shale pyrolysis was established. The results obtained will be of help for a better understanding of the nitrogen conversion process. Moreover, it was found that when improving operational parameters and using some reactants to remove harmful intermediates formed in the decomposition process of oil shale, the movement of nitrogen-containing species into shale oil may be hindered and thus its quality improved.

## 2. Experiments on organic nitrogen conversion during oil shale retorting

Experiments on organic nitrogen conversion during retorting Huadian oil shale (Type I kerogen) in a fixed bed reactor were performed and the results analyzed in the authors' previous works [3–7], which showed that respectively 61.3, 26.2 and 12.5% of organic nitrogen present in oil shale remained in semicoke, shale oil and non-condensable gases. Using electro-spray ionization Fourier transform ion cyclotron resonance mass spectrometry (ESI FT-ICR MS) [5], it was established that the basic nitrogen classes present in shale oil were identified as  $N_1$ ,  $N_1O_1$ ,  $N_1O_2$ ,  $N_1O_3$ ,  $N_1S_1$  and  $N_2$ , among which  $N_1$  and  $N_1O_1$  classes accounted for about 80%. ESI FT-ICR MS and gas chromatography-mass spectrometry (GC-MS) disclosed that the major organic nitrogen components extracted from oil shale semicoke were  $C_{24}H_{15}N_2$ ,  $C_{21}H_{19}N_2O_2$ ,  $C_{20}H_{15}N_2O_3$  and  $C_{18}H_{35}ON$ . Employing the MRU Vario Plus industrial flue gas analyzer and the Gasetm DX-4000 FTIR gas analyzer, it was found that nitrogen species in non-condensable gases existed in the form of  $NO_x$  besides  $NH_3$ , as shown in Figure 1. It is important to note that  $N_2$  and HCN gases were not obtained because  $N_2$  could not be identified by these two gas analyzers and HCN was not calibrated into the FTIR gas analyzer at that time. These experimental results demonstrated that nitrogen-containing species present in oil shale retorting products were more numerous than raw nitrogen species in unprocessed oil shale. Therefore in this work, the conversion of raw organic nitrogen during the retorting of oil shale was investigated using the quantum chemical transition state theory.

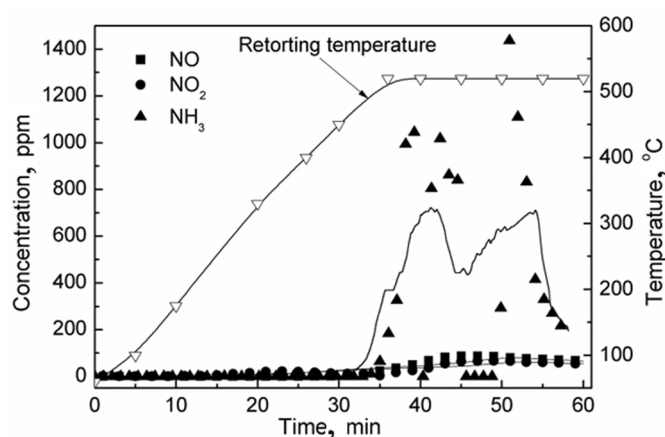


Fig. 1.  $NO_x$  and  $NH_3$  emissions from the retorting of Huadian oil shale (smoothed by the adjacent averaging).

### 3. Computational details

#### 3.1. Physical models

The physical models of main nitrogen-containing species, including indole, pyridine, quinoline, carbazole and amide, were created according to the structural characteristics of Huadian oil shale kerogen [3, 7]. To reduce the computational cost, the modeled structures were simplified (Fig. 2) based on the following assumptions:

- 1) All the structures modeled are part of the kerogen matrix, and the length of the carbon chain branched to the functional groups is reduced to three atoms since those atoms which are further than the  $\gamma$  position have a little influence on the chemical reactions of functional groups [13].
- 2) The effects of the other parts of the kerogen matrix on the course of the calculated reactions are not taken into account during the theoretical modeling.

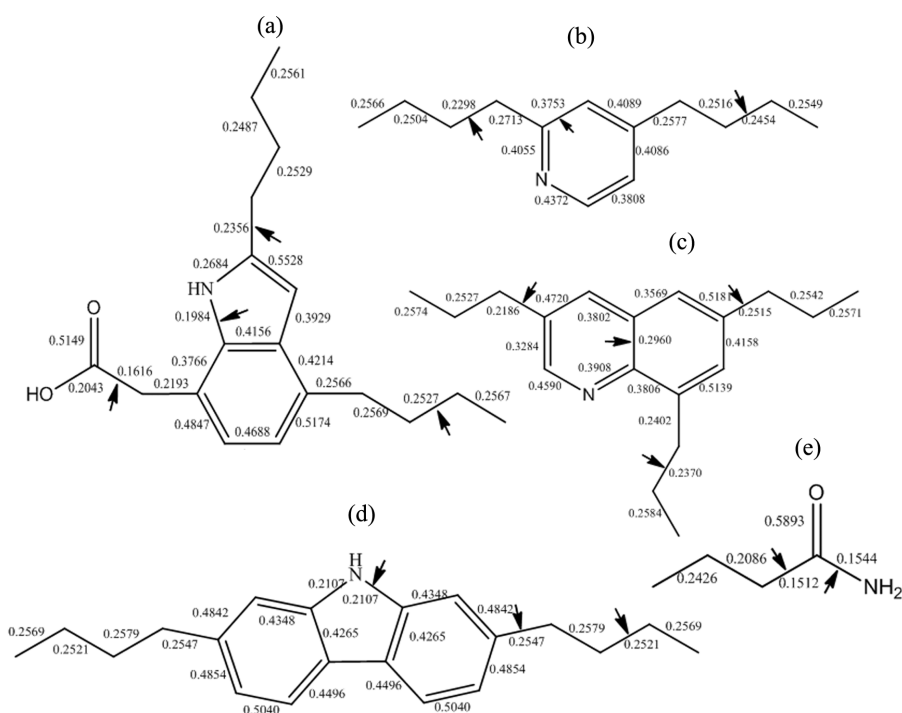


Fig. 2. Mulliken analysis of nitrogen-containing species in Huadian oil shale kerogen: (a) indole, (b) pyridine, (c) quinoline, (d) carbazole, (e) amide.

#### 3.2. Theoretical methods

Spin contamination is extremely important to be considered especially in case of radical systems and calculated energy. In this paper, the B3LYP

method [14] with the 6-31G (d) basis set [15, 16] (B3LYP/6-31G (d)), which is advantageous for its small and acceptable spin contamination [17, 18], was used for the structural optimization of all the reactants, intermediates and main products. In addition, the same method and basis set were applied to the vibrational analysis of the proposed structures to find out whether these were either equilibrium structures or transition state structures [18]. Intrinsic reaction coordinate (IRC) calculations for all the transition state structures were also carried out to confirm that they led to the desired reactants and products [18]. To ensure the accuracy of the calculated energies, zero-point energies were included in the theoretical results and all the energies were rectified with a scale factor of 0.9804 which corresponds to the 6-31G (d) basis set [19]. The Gaussian 09, Revision A.02 package was employed in this work.

#### 4. Results and discussion

The established decomposition mechanisms of nitrogen-containing species in oil shale kerogen are shown in Figures 3 and 4, and the relative energies for each pathway are given in Table.

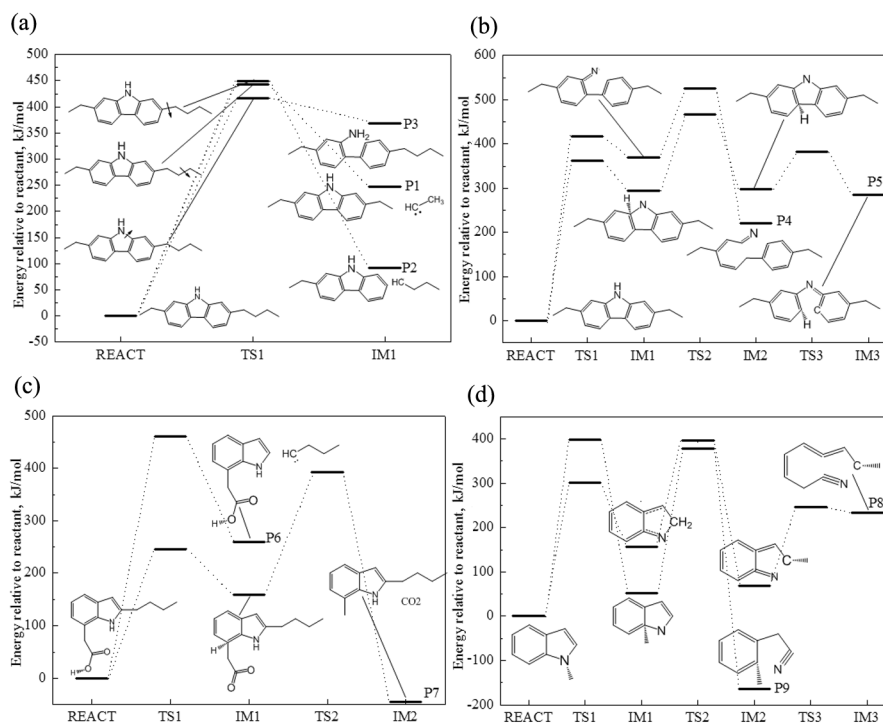


Fig. 3. Chemical reaction pathways of thermal decomposition of pyrrolic nitrogen. (Abbreviations used: REACT – reactant,  $P_n$  – pathway,  $TS_n$  – transition state,  $IM_n$  – intermediate.)

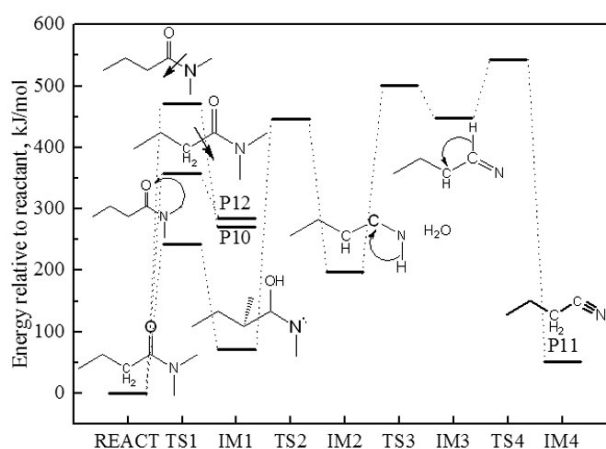


Fig. 4. Chemical reaction pathways of thermal decomposition of amide nitrogen. (Abbreviations used: REACT – reactant, P $n$  – pathway, TS $n$  – transition state, IM $n$  – intermediate.)

**Table. Energies relative to the reactant in the speculated reaction pathways, kJ/mol**

P	REACT	TS1	IM1	TS2	IM2	TS3	IM3	TS4	IM4
P1	0.0	443.5	247.5						
P2	0.0	449.6	91.7						
P3	0.0	416.0	368.9						
P4	0.0	416.0	368.9	526.3	220.3				
P5	0.0	362.1	293.3	467.3	297.1	381.5	285.2		
P6	0.0	460.7	259.6						
P7	0.0	245.9	159.5	392.5	-44.9				
P8	0.0	301.7	157.4	397.6	69.2	245.7	234.3		
P9	0.0	397.7	52.6	379.0	-163.8				
P10	0.0	358.4	284.9						
P11	0.0	243.6	71.4	447.1	197.5	500.3	448.4	542.4	50.6
P12	0.0	471.3	271.3						

Abbreviations used: P $n$  – pathway ( $n = 1, 2, \dots, 12$ ); REACT – reactant; TS $n$  – transition state; IM $n$  – intermediate/product.

#### 4.1. Conversion of pyrrolic nitrogen

As is well known, the cleavage of aromatic rings is much more difficult to occur than that of aliphatic carbon chains. Using the Mulliken analysis, according to which the lower the Mulliken population, the weaker the corresponding bond [20], the most probable rupture point during the decomposition can be obtained. The Mulliken analysis of pyrrolic nitrogen groups (Figs. 2a and 2d) demonstrated that the rupture points in their structures were the C–C bond at the  $\gamma$ -,  $\beta$ - and  $\alpha$ -positions of the branched aliphatic carbon chains and the C–N bond in the pyrrolic nitrogen rings. The corresponding chemical reaction pathways of the cleavage of these rings are shown in Figure 3, and the energies of the reactants are given in Table.

#### 4.1.1. Carbazole conversion

In this paper, for carbazole species five reaction pathways were found, which are depicted in Figures 3a and 3b. The activation energy ( $E_a$ ) for the cleavage of the C–C bond at positions  $\gamma$  (pathway P1) and  $\alpha$  (pathway P2) of the branched aliphatic carbon chains is 443.5 and 449.6 kJ/mol, respectively, meaning that the C–C bond cleavage at the former position takes place first during the heating. However, the  $E_a$  for the cleavage of the C–N bond (pathways P3 and P4) in the pyrrolic ring is about 416 kJ/mol, being lower than that for the cleavage of the C–C bond at position  $\gamma$ . So, the cleavage of the C–N bond in the pyrrolic ring takes place first during the thermal decomposition of kerogen, followed by the cracking of the C–C bond at position  $\gamma$ . During the further decomposition of the intermediates formed, the cleavage of the C–C bond at position  $\alpha$  occurs to form some nitrile and/or amino species and their derivatives. These new nitrogen-containing species, such as octadecanenitrile ( $C_{18}H_{35}N$ ) and heptadecanenitrile ( $C_{17}H_{33}N$ ), were found in the intermediates and main products from the retorting of Huadian oil shale. The comparison of  $E_a$  of reaction pathways P1–P4 with that of pathway P5 (see Table) suggests that the latter pathway should easily take place due to its lower  $E_a$ . However, considering the absence of possible intermediates and main products from pathway P5 in oil shale pyrolytic products, it is likely not to come about in the actual oil shale pyrolysis.

#### 4.1.2. Indole conversion

Indole is another type of pyrrolic nitrogen in oil shale kerogen. There are three carbon chains branched to the indole species according to the kerogen model. On the basis of the Mulliken analysis of the indole structure (Fig. 2a), there are four possible fracture points during oil shale pyrolysis: 1) C–C bond at position  $\gamma$  in the carbon chain branched to the aromatic ring, 2) C–C bond at position  $\alpha$  in the carbon chain branched to the pyrrole ring, 3) C–C bond at position  $\beta$  near the carboxylic acid species, and 4) C–N bond in the pyrrolic ring. The related chemical reaction pathways are shown in Figures 3c and 3d.

From Figures 3c and 3d it is seen that the  $E_a$  for the cleavage of the C–C bond at position  $\alpha$  in the carbon chains branched to the aromatic ring is 460.7 kJ/mol (pathway P6), which is a little higher than the  $E_a$  for the C–C bond cleavage at position  $\gamma$ . At the same time, the  $E_a$  for the cleavage of the C–C bond at position  $\beta$  (pathway P7) near the carboxylic acid species to produce  $CO_2$  is 392.5 kJ/mol. So, it can be expected that carboxylic acid will decompose earlier than the branched aliphatic carbon chains. When it comes to the decomposition of the pyrrolic ring (pathways P8 and P9), the C–N bond far from the aromatic ring is the weakest in the pyrrolic ring, the direct crack of which has the  $E_a$  of 301.7 kJ/mol, which is the lowest among all the calculated reaction pathways. So, it can be concluded that the cracking of the pyrrolic ring at the C–N bond to form nitriles is most likely to happen for the indole species during oil shale pyrolysis. After that, the cracking of the C–C

bond in the branched carbon chains takes place to form unsaturated carbon chains or some other products (carboxylic acids or CO<sub>2</sub>).

From the results discussed above it is clear that both carbazole and indole species crack earlier at the C–N bond than at the other points. However, this C–N bond still shows a thermal stability with high activation energy. So, it is considered that most of the carbazole and indole species should be evaporated into shale oil or attacked by some unsaturated hydrocarbon radicals to form nitriles and its derivatives during the low-temperature pyrolysis of oil shale rather than crack directly [21].

#### 4.2. Conversion of pyridinic nitrogen

Pyridinic nitrogen in coal and oil shale is mainly present in the form of pyridine and quinoline and their derivatives. There have been conducted many investigations on the thermal conversion of this type of nitrogen in coal [10, 22–24]. It has been found that the energy barrier for the direct cracking of these pyridinic rings is about 600 kJ/mol and that the conversion starts at a temperature of 700 °C and becomes more intensive at 1200 °C. While attacked by H radicals under low-temperature conditions (about 600 °C), pyridinic nitrogen can also be partly converted into nitriles [21]. However, this conversion does not proceed easily in the conventional oil shale retorting process whose final temperature is usually below 550 °C. As a result, only a small part of pyridinic nitrogen can be converted during the retorting of oil shale, while the majority of the compound remains in its original state in the solid residue or evaporates into downstream products, such as 1-(2-benzyloxyethyl)-1,2,3,6-tetrahydropyridine and 2-methylpyridine [4–6]. But upon further utilization of the solid residue, e.g. combustion and gasification, these organic nitrogen species may convert to N-containing gases according to the mechanisms described earlier [22–24].

#### 4.3. Conversion of amino nitrogen

The amino nitrogen in the kerogen of Huadian oil shale is mainly present in two forms: the amide species and the amino species bonded to the aliphatic carbon chains [7]. The pyrolysis properties of these two species are not similar because of the direct influence of the nearby oxygen atom on the amide species [13]. The amino species bonded to the aliphatic carbon chains alone are more likely to be converted into hydrocarbon radicals and amino radicals which will be further pyrolyzed into alkenes and NH<sub>3</sub> emissions. At the same time, the thermal decomposition mechanism of amide species becomes more complex.

The possible reaction pathways of amide species during the pyrolysis are shown in Figure 4. The energy barrier for the cracking of the C–C bond to form amides and alkenes (pathway P12) is 471.3 kJ/mol, while the energy barrier of the direct cracking of the C–N bond to form hydrocarbon and amino radicals (pathway P10) is just 358.4 kJ/mol, which means that the amide species are more likely to directly crack into hydrocarbon and amino

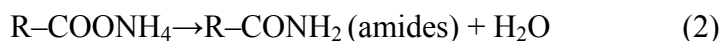
radicals during oil shale pyrolysis. As for the decomposition of these species to form water and nitriles (pathway P11), the  $E_a$  is 542.4 kJ/mol, which is obviously higher than that of the direct cracking of the C–N bond to form hydrocarbon and amino radicals.

From the above it is clear that the chemical reaction pathway most likely to happen is the direct cracking of the C–N bond to form hydrocarbon and amino radicals. While further pyrolyzed and attacked by some other radicals (H radicals, hydrocarbon radicals, etc.), these radicals could be easily converted into alkenes or alkanes and  $\text{NH}_3$  emissions, as shown in Figure 1.

#### 4.4. Mechanisms of further nitrogen conversion

From the conversions of pyrrolic, pyridinic and amino nitrogen it is obvious that most of the organic nitrogen converts into nitrile or amino species which are regarded as the main precursors of nitrogen-containing products. However, all these conversions require a higher  $E_a$  than 300 kJ/mol, meaning that the direct decomposition of nitrogen-containing species should take place at higher pyrolysis temperatures. This conclusion is also supported by Aho et al. [21], who ascertained that the direct decomposition of nitrogen-containing rings became more intensive when the temperature reached 800 °C. On the other hand, these nitrogen-containing species might not intensively decompose during traditional oil shale retorting at lower operational temperatures. Besides the direct decomposition of organic nitrogen species, nitrogen-containing rings may be attacked by the surrounding radicals such as the H radical to form nitriles, while this process may take place easily at lower pyrolysis temperatures [25].

Following the initial conversion of organic nitrogen species, some of the resulting nitrogen-containing intermediates are further decomposed into HCN/ $\text{NH}_3$  emissions. While colliding with oxygen-containing species or radicals, these nitrogen-containing intermediates and products are converted into  $\text{NO}_x$ , which explains the appearance of  $\text{NO}_x$  emissions during the retorting of oil shale (see Fig. 1). At the same time,  $\text{NH}_3$  would also partly react with carboxylic acids to form nitrile species, while ammonium salts of carboxylic acid ( $-\text{COONH}_4$ ) and amides ( $-\text{CONH}_2$ ) are formed as intermediates [26]. These processes can be described as follows:



This conversion process can be validated by several proofs. First, the similarity in structure between carboxylic acids ( $-\text{COOH}$ ), amides ( $-\text{CONH}_2$ ) and nitrile species ( $-\text{CN}$ ) was established by the GC-MS analysis of bitumen and oil shale semicoke extracts during the experimental work. Second, there was a slight increase in the quaternary nitrogen content in bitumen compared with the kerogen matrix [4]. According to this, the

amount of nitrile species in shale oil might be reduced by decreasing that of carboxylic acids during oil shale retorting. If increasing the pyrolysis temperature further, these reactions might be accelerated and  $\text{NO}_x$  gases would reach their maximum at about  $800^\circ\text{C}$  [21].

As concluded above, because of the high  $E_a$  of these decomposition reaction pathways, the thermal conversion of nitrogen-containing species should mainly result from the attack of some radicals during the retorting of oil shale. At the same time, most nitrogen-containing species remain in the solid residues or evaporate into downstream products (shale oil, bitumen or gases emissions) along with the cracking of the kerogen matrix. This is in good agreement with the experimental results which demonstrate that more than half of the kerogen matrix organic nitrogen still remains in oil shale semicoke during the retorting ( $< 520^\circ\text{C}$ ). However, most nitrogen species have changed their state and may be subjected to further conversion if the pyrolysis temperature is increased. A detailed nitrogen species conversion mechanism during oil shale retorting is shown in Figure 5.

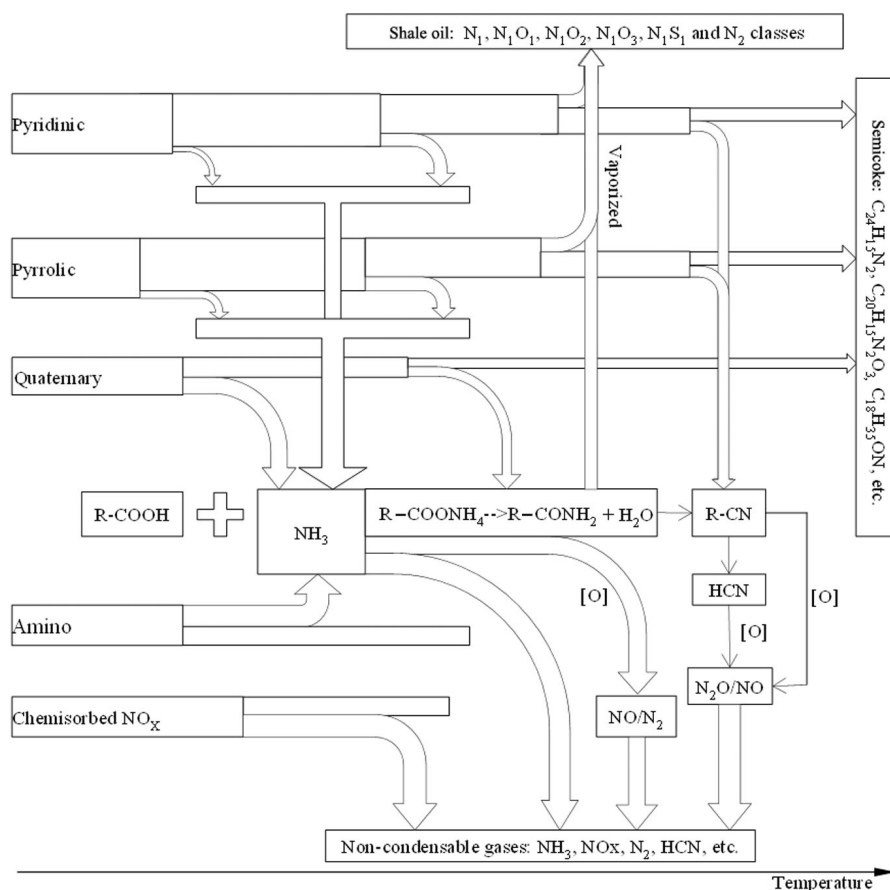


Fig. 5. History of conversion of nitrogen groups with increasing temperature.

## 5. Conclusions

This work is a further investigation of the thermal decomposition of oil shale kerogen. The authors summarized the experimental results on organic nitrogen conversion of Huadian oil shale, and constructed models for describing the decomposition of nitrogen-containing species of the oil shale kerogen matrix by using the transition state theory in the Gaussian 09. Revision A.02 package. The main conclusions can be drawn as follows:

1. The pyridinic and pyrrolic rings in the initial nitrogen-containing organic matter of oil shale crack into nitrile or amino species, and amino nitrogen converts into  $\text{NH}_3$ , while all these processes require a high energy input. Compared with the direct decomposition reactions, the conversion of more nitrogen-containing species should result from the attack of some radicals (H and aliphatic radicals, etc.), forming nitrile and amino species at lower pyrolysis temperatures.
2. The nitrile and amino species may further decompose into HCN and  $\text{NH}_3$  emissions, respectively. Some portion of  $\text{NH}_3$  may also react with the remaining carboxylic acids to form nitriles in this process.
3. If further attacked by oxygen-containing groups, HCN and/or  $\text{NH}_3$  and their precursors (nitrile and amino species) may form  $\text{NO}_x$  during the retorting of oil shale.
4. In the traditional oil shale retorting at low pyrolysis temperatures, most nitrogen species remain in oil shale semicoke. However, the majority of them have changed their state, and may further undergo conversion according to the mechanisms described if the pyrolysis temperature is increased.

## Acknowledgement

This work was sponsored within the framework of the Shanghai Pujiang Program of China (Grant No. 15PJD018).

## REFERENCES

1. Mitra-Kirtley, S., Mullins, O. C., Branthaver, J. F., Cramer, S. P. Nitrogen chemistry of kerogens and bitumens from X-ray absorption near-edge structure spectroscopy. *Energ. Fuel.*, 1993, **7**(6), 1128–1134.
2. Kelemen, S. R., Afeworki, M., Gorbaty, M. L., Kwiatek, P. J., Solum, M. S., Hu, J. Z., Pugmire, R. J. XPS and  $^{15}\text{N}$  NMR study of nitrogen forms in carbonaceous solids. *Energ. Fuel.*, 2002, **16**(6), 1507–1515.
3. Tong, J. H., Han, X. X., Wang, S., Jiang, X. M. Evaluation of structural characteristics of Huadian oil shale kerogen using direct techniques (solid-state  $^{13}\text{C}$  NMR, XPS, FT-IR, and XRD). *Energ. Fuel.*, 2011, **25**(9), 4006–4013.

4. Li, Q. Y., Han, X. X., Liu, Q. Q., Jiang, X. M. Thermal decomposition of Huadian oil shale. Part 1. Critical organic intermediates. *Fuel*, 2014, **121**, 109–116.
5. Tong, J. H., Liu, J. G., Han, X. X., Wang, S., Jiang, X. M. Characterization of nitrogen-containing species in Huadian shale oil by electrospray ionization Fourier transform ion cyclotron resonance mass spectrometry. *Fuel*, 2013, **104**, 365–371.
6. Han, X. X., Jiang, X. M., Cui, Z. G., Liu, J. G., Yan, J. W. Effects of retorting factors on combustion properties of shale char. 3. Distribution of residual organic matters. *J. Hazard. Mater.*, 2010, **175**(1–3), 445–451.
7. Tong, J. H., Jiang, X. M., Han, X. X., Wang, X. Y. Evaluation of the macromolecular structure of Huadian oil shale kerogen using molecular modeling. *Fuel*, 2016, **181**, 330–339.
8. Oh, M. S., Taylor, R. W., Coburn, T. T., Crawford, R. W. Ammonia evolution during oil shale pyrolysis. *Energ. Fuel.*, 1988, **2**(1), 100–105.
9. Zhai, L., Zhou, X. F., Liu, R. F. A theoretical study of pyrolysis mechanisms of pyrrole. *J. Phys. Chem.*, 1999, **103**(20), 3917–3922.
10. Ling, L. X., Zhang, R. G., Wang, B. J., Xie, K. C. Pyrolysis mechanisms of quinoline and isoquinoline with density functional theory. *Chinese J. Chem. Eng.*, 2009, **17**(5), 805–813.
11. Ninomiya, Y., Dong, Z. B., Suzuki, Y., Koketsu, J. Theoretical study on the thermal decomposition of pyridine. *Fuel*, 2000, **79**(3–4), 449–457.
12. Wójtowicz, M. A., Pels, J. R., Moulijn, J. A. The fate of nitrogen functionalities in coal during pyrolysis and combustion. *Fuel*, 1995, **74**(4), 507–516.
13. Zhang, Z. X., Hang, T. J., Yuan, Y. Z. *Spectral Analysis of Organics*. People's Medical Publishing Press, Beijing, 2009 (in Chinese).
14. Becke, A. D. A new mixing of Hartree-Fock and local density-functional theories. *J. Chem. Phys.*, 1993, **98**(2), 1372–1377.
15. Lee, C., Yang, W., Parr, R. G. Development of the Colle-Salvetti correlation-energy formula into a functional of the electron density. *Phys. Rev. B*, 1988, **37**(2), 785–789.
16. Miehlich, B., Savin, A., Stoll, H., Preuss, H. Results obtained with the correlation energy density functionals of Becke and Lee, Yang and Parr. *Chem. Phys. Lett.*, 1989, **157**(3), 200–206.
17. Perry, S. T., Hambly, E. M., Fletcher, T. H., Solum, M. S., Pugmire, R. J. Solid-state <sup>13</sup>C NMR characterization of matched tars and chars from rapid coal devolatilization. *P. Combust. Inst.*, 2000, **28**(2), 2313–2319.
18. García, P., Espinal, J. F., Martínez de Lecea, C. S., Mondragón, F. Experimental characterization and molecular simulation of nitrogen complexes formed upon NO-char reaction at 270 °C in the presence of H<sub>2</sub>O and O<sub>2</sub>. *Carbon*, 2004, **42**(8–9), 1507–1515.
19. Foresman, J. B., Frisch, A. E. *Exploring Chemistry with Electronic Structure Methods: A Guide to Using Gaussian*, 2nd Ed. Gaussian, 1996.
20. Qiu, L., Xiao, H. M., Ju, X. H., Gong, X. D. Theoretical study on the structures and properties of bicyclo-HMX. *Acta Chim. Sinica*, 2005, **63**(5), 377–384.
21. Aho, M. A., Hämäläinen, J. P., Tummavuori, J. L. Conversion of peat and coal nitrogen through HCN and NH<sub>3</sub> to nitrogen oxides at 800 °C. *Fuel*, 1993, **72**(6), 837–841.

22. Yuan, S., Li, J., Zhou, Z. J., Wang, F. C. Mechanisms of HCN and NH<sub>3</sub> formation during rapid pyrolysis of pyridinic nitrogen containing substances. *J. Fuel Chem. Technol.*, 2011, **39**(6), 413–418 (in Chinese with English abstract).
23. Kambara, S., Takarada, T., Toyoshima, M., Kato, K. Relation between functional forms of coal nitrogen and NO<sub>x</sub> emissions from pulverized coal combustion. *Fuel*, 1995, **74**(9), 1247–1253.
24. Ogunsola, O. M. Decomposition of isoquinoline and quinoline by supercritical water. *J. Hazard. Mater.*, 2000, **74**(3), 187–195.
25. Li, C. Z., Tan, L. L. Formation of NO<sub>x</sub> and SO<sub>x</sub> precursors during the pyrolysis of coal and biomass. Part III. Further discussion on the formation of HCN and NH<sub>3</sub> during pyrolysis. *Fuel*, 2000, **79**(15), 1899–1906.
26. Evans, R. J., Batts, B. D., Cant, N. W., Smith, J. W. The origin of nitriles in shale oil. *Org. Geochem.*, 1985.

*Presented by A. Siirde*

Received March 9, 2015